*Cosmic Masers: Proper Motion toward the Next-Generation Large Projects*
*Proceedings IAU Symposium No. 380, 2024*
*T. Hirota, H. Imai, K. Menten, & Y. Pihlström, eds.*
doi:10.1017/S1743921323002594

# Maser Tracers of Gas Dynamics near Young Stars New Perspectives

**Alberto Sanna**[1] **and Luca Moscadelli**[2]

[1]INAF, Osservatorio Astronomico di Cagliari, via della Scienza 5, 09047, Selargius, Italy.
email: alberto.sanna@inaf.it

[2]INAF, Osservatorio Astrofisico di Arcetri, Largo E. Fermi 5, 50125 Firenze, Italy

**Abstract.** The protostellar environment where young stars form has physical conditions suitable to excite a number of molecular maser lines that have traditionally provided an unique probe of star formation kinematics, at the highest angular resolution of radio very long baseline interferometry (VLBI) observations. In the following, we will discuss a number of recent results on our understanding of the gas dynamics traced by masers in the vicinity of young forming stars. These findings provide direct clues on how our community can substantially contribute to the field of star formation in the next decade.

**Keywords.** Masers, Stars: formation, ISM: kinematics and dynamics

## 1. Introduction

The protostellar environment where young stars form has physical conditions suitable to induce population inversions between specific pairs of energy levels in several abundant molecules, including water ($H_2O$), methanol ($CH_3OH$), hydroxyl (OH), ammonia ($NH_3$), silicon monoxide (SiO), and formaldehyde ($H_2CO$). The resulting non-thermal maser emission in the corresponding spectral transitions provides a beacon whose brightness temperature (typically $> 10^8$ K) far exceeds that of the more commonly-excited thermal emission lines. Maser maps typically show a large number of bright and compact spots that mark parcels of gas (or cloudlets) where amplified emission is beamed almost along the line-of-sight. Their enhanced brightness temperature has provided the sole target for spectroscopic Very Long Baseline Interferometry (VLBI) observations, whose milli-arcsecond beam size is inversely proportional to the expected measurement sensitivity. Consequently, since early '80 (e.g., Genzel *et al.* 1981; Gwinn *et al.* 1992), iterated VLBI observations of maser spots, which are excited in the inner circumstellar regions ($\lesssim 1000$ au), have been used to trace the displacement in time of individual cloudlets (namely, their proper motions), which, together with the doppler-shift of the maser lines, provide the full-space motion of local gas. In this context, maser lines have traditionally provided an unique probe of star formation, so far at centimeter wavelengths especially.

When talking about gas dynamics near young forming stars, one commonly is reminded of two major dynamical structures, namely, what we generally call *disk-like structures* and the *jets and winds* launched from these circumstellar regions. In the literature, two molecular masers, water and methanol, have traditionally been used to study these complementary environments, whose association with either one or the other maser species directly follows from the different excitation mechanisms. Firstly, water masers in the 22.2 GHz transition, whose pumping mechanism is predominantly collisional, were identified as tracer of shock phenomena in the vicinity of stars (e.g., Elitzur *et al.* 1989, 1992; Kaufman & Neufeld 1996; Hollenbach *et al.* 2013), either very young or evolved, and

their observations has been key to reveal the dynamics of fast shocked layers of ejected gas, even in exceptional environments such as magneto-hydrodynamic disk winds (e.g., Moscadelli *et al.* 2022). Subsequently, methanol masers in the 6.7 GHz transition, whose pumping mechanism is predominantly radiative, were identified as tracer of warm and quiescent gas in the inner (massive) circumstellar regions where the requirements of an IR field and high methanol column densities are satisfied (e.g., Cragg *et al.* 1992, 2005; Sobolev *et al.* 1997).

In the following, we are going to highlight some recent results related to our understanding of water and methanol masers in star formation, and their local environments, whose developments allow us to draw a number of useful predictions for maser observations with next generation facilities, such as the next-generation VLA (ngVLA) and the Square Kilometer Array (SKA).

## 2. Water masers associated with proto-stellar jets and winds

### 2.1. *The POETS survey*

Since the last maser symposium, we have spent much efforts on a large maser project called POETS, which stands for the "Protostellar Outflows at the EarliesT Stages" survey. This project has been grounded on a survey of combined water masers and radio continuum observations at the highest angular resolution available towards a large number of young and massive stars, which we have presented in a series of papers between 2018 and 2020, with a pilot study in 2016 (Sanna *et al.* 2018, 2019b; Moscadelli *et al.* 2016, 2019, 2020).

In Fig. 1, we present an example of the type of studies we did, by mapping the water maser distribution (and motions) relative to the position and morphology of the ionised gas around each target of the sample, that had to fulfill four requirements:

- star-forming sites showing evidence of being prior to an ultra-compact H II region phase, which statistically means that a source is typically younger than ten-thousand years;
- massive regions, with luminosities of several thousands times that of our Sun;
- targets associated with bright 22.2 GHz $H_2O$ masers, with flux densities of several tens of Jy and rich spectra of several distinct maser features;
- targets having accurate trigonometric distance measurements, belonging to the "Bar and Spiral Structure Legacy Survey" (Reid *et al.* 2014).

For our final sample of 36 targets, the dataset was made up of: 1) phase-referencing, multi-epoch, Very Long Baseline Array (VLBA) spectral line observations at 22 GHz, and 2) Very Large Array (VLA) continuum observations conducted at three frequency bands, 6, 15, and 22 GHz in the A- and B-array configurations, with sensitivities down to a few $\mu$Jy beam$^{-1}$.

Water maser and continuum emissions allow us to trace fast shocked layers of gas and (thermal) free-free from ionized material of jets and winds, the latter generally referred to as "radio thermal jets". For each target, we aimed to quantify the morphology and dynamics of primary outflows, where primary outflows are those whose material is initially (gravitationally) bound to the driving star.

### 2.2. *Results: correlation among luminosities*

A first general result of POETS follows from a comparison of the (isotropic) water maser luminosity with respect to the radio continuum luminosity of the targets. In Fig. 2 (left), one can appreciate a strong linear correlation between these two quantities, which

https://doi.org/10.1017/S1743921323002594 Published online by Cambridge University Press

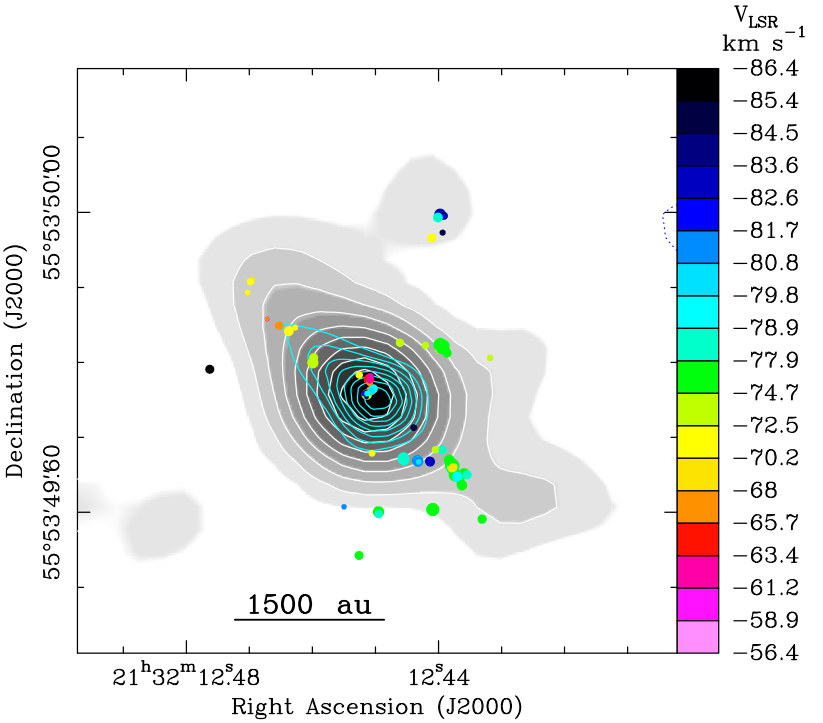


**Figure 1.** Example of POETS observations for the target source G097.53+03.18. This map shows a typical combination of radio continuum emission, with grey shades and cyan contours for 12 and 22 GHz emission respectively, and 22.2 GHz water maser cloudlets, marked with colored dots according to the line-of-sight velocity scale to the right. Adapted from Moscadelli *et al.* (2016).

is also associated with a one-to-one detection rate of faint ($\lesssim 100\mu$Jy) radio continuum emission towards water masers sites.

This correlation can be better understood when looking at a second correlation (Fig. 2, right), that between the same radio continuum luminosity and the bolometric luminosity of the source, where only targets whose luminosity is dominated by a single object have been considered. In this well-known diagram, the Lyman curve sets the level of radio luminosity that can be produced by Lyman photons from a young star of a given spectral type, which have energies high enough to ionize hydrogen atoms. At a first order, this curve divides the stellar population into low-mass objects to the left and high-mass objects to the right of the plot. The fact that low-mass objects cannot photo-ionize their associated radio continuum, it has long been recognized as evidence of a shock ionization mechanism at work, and this dependence yields the observed linear trend.

The fact that the same linear correlation extends also at higher star masses, for young stars associated with water masers, suggests the following conclusion – *compact radio continuum emission associated with $H_2O$ masers is dominated by shock ionization*. From this evidence, a first corollary would state that, by means of next-generation centimeter interferometers, we expect to simultaneously detect, at milli-arcsecond resolution, masers and (thermal) continuum that are spatially coincident, allowing for an accurate registration of their relative positions.

https://doi.org/10.1017/S1743921323002594 Published online by Cambridge University Press

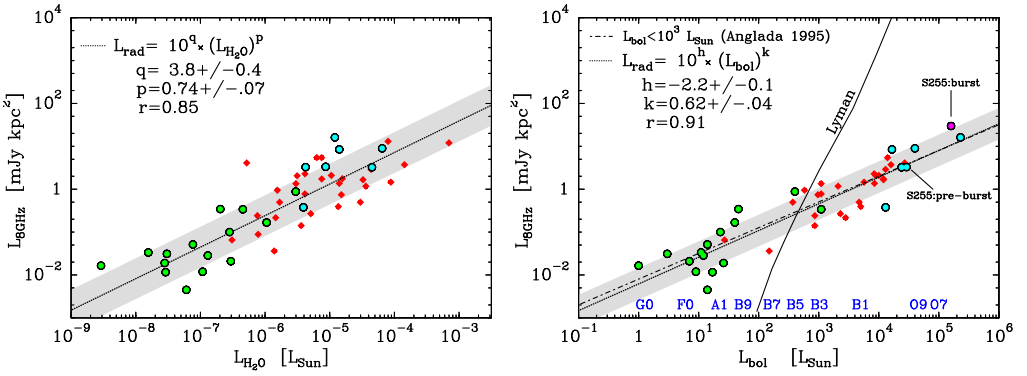


**Figure 2.** Dependence of the radio luminosity of the POETS sample on the $H_2O$ maser (left) and bolometric (right) luminosities. Red diamonds mark sources from the POETS sample, cyan circles are used for a number of prototypical radio thermal jets, and green circles for low-luminosity $H_2O$ maser sites. In both panels, the dotted bold line traces the $\chi^2$ fit to the sample distribution with the $1\,\sigma$ dispersion in grey (fit parameters and uncertainties on top left). In the right panel, the solid line traces the ionized flux expected from the Lyman continuum of ZAMS stars earlier than B8 and spectral types, corresponding to a given luminosity, are indicated in blue near the lower axis. More details in Fig. 5 of Sanna *et al.* (2018).

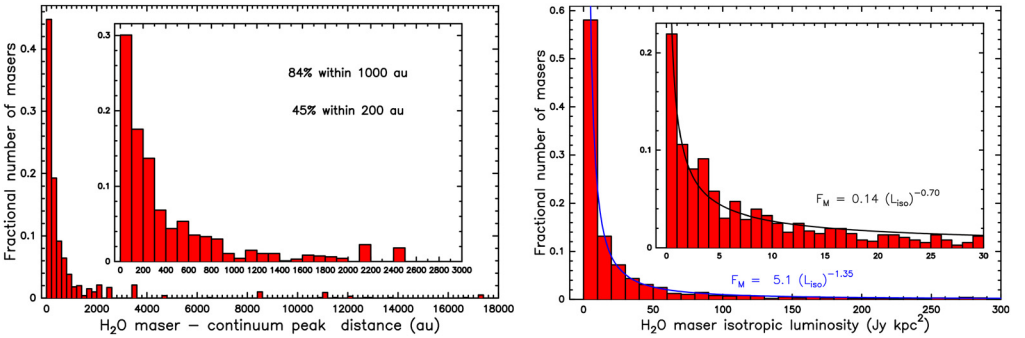


**Figure 3.** Normalized histograms of the number of $H_2O$ masers found at different distances from their stars (left) and with respect to their intrinsic brightness (right). Adapted from Moscadelli *et al.* (2020).

### 2.3. *Results: distribution of $H_2O$ masers from the star position*

A second general result of POETS follows from the spatial distribution of water maser cloudlets with respect to the position of the nearby radio continuum peak, generally assumed to pinpoint the young star position when its spectral index is partially optically thick. In the left panel of Fig. 3, we built up a histogram of the number of $H_2O$ masers found at different distances from their stars, considering either spatial scales of several 1000 au (outer plot) and the inner few 1000 au (inset) from the origin. This distribution exponentially increases when the distance from the radio continuum peak decreases, allowing us to statistically state that – *about 80% of the observed water maser cloudlets are found within 1000 au of their associated star, and almost half of them within only a few 100 au.*

Alternatively, this evidence suggests that a given water maser distribution can be used as an accurate proxy of the star position, whenever a significant number of maser cloudlets are detected. Notably, this statistical result, derived for the first time by means of high-resolution and high-sensitivity observations, is at variance with past claims that water masers are sampling large distances of several 1000 au from their associated star.

https://doi.org/10.1017/S1743921323002594 Published online by Cambridge University Press

### 2.4. *Results: a $H_2O$ maser brightness function – how many maser spots are we missing?*

A third general result of POETS follows from the analysis of the number of water maser detections as a function of their intrinsic brightness, plotted in terms of their isotropic (normalized) luminosity. Their histogram in the right panel of Fig. 3 shows an exponential increase which sharply peaks towards low maser luminosities, similarly to the left panel.

The conclusion of this statistical analysis has a direct implication for our spectroscopic VLBI observations, meaning that – *at sub-mJy sensitivities, we expect to double the current number of $H_2O$ maser detections, that rely on sensitivities an order of magnitude higher.* Alternatively, the combined results of Sect. 2.3 and 2.4 suggest another useful corollary for next-generation centimeter interferometers, that will open up a new era of water maser observations, allowing us to study new phenomena very close to massive young stellar objects (e.g., Moscadelli *et al.* 2022).

## 3. Methanol masers associated with proto-stellar disk-like structures

Since their discovery in the early '90 (Menten 1991), methanol masers at 6.7 GHz have been associated with the innermost gas surrounding young stars several times more massive than our Sun, due to the physical conditions predicted for the maser excitation (e.g., Cragg *et al.* 2005). A typical methanol maser spectrum at 6.7 GHz shows spectral features within about 10 $\mathrm{km\,s^{-1}}$ from the systemic velocity of nearby gas, suggesting that methanol masers are kinematic tracers of more quiescent gas than water masers are. This characteristic property has a counterpart in the milli-arcsecond regular structure of 6.7 GHz maser cloudlets which persists over many years (Minier *et al.* 2002; Sanna *et al.* 2010a; Moscadelli *et al.* 2011b). Proper motion measurements of 6.7 GHz maser cloudlets published since 2010 have confirmed velocity components on the plane-of-the-sky of the same magnitude of the line-of-sight velocities (Sanna *et al.* 2010a,b).

In the years, following this evidence, methanol masers have been generally referred to be associated with "disk-like structures", although this definition is vague and does not provide specific clues about the environment where masers are excited. For instance, if $CH_3OH$ masers are expected to be quenched above volume densities of approximately $10^8\,\mathrm{cm^{-3}}$, they would not be excited in the inner few 100 au of young and massive stars where gas likely attains Keplerian equilibrium, but would only arise in the less dense outskirts where a slower rotating envelope (or toroid) is predicted. In this respect, are 6.7 GHz maser proper motions consistent with these expectations and what have we learned in the past decade?

In the following, we want to highlight some guidelines for future studies of methanol masers at 6.7 GHz that can be useful to improve our definition of "disk-like" environment.

### 3.1. *Physical conditions of methanol maser gas*

A first instructive example comes from a well-known star-forming region, G023.01–00.41, and the environment surrounding its most massive star ($\sim 20\,\mathrm{M_\odot}$). In Fig. 4, we show the appearance of its disk-like structure as imaged with the Atacama Large Millimeter Array (ALMA) by means of a methanol line near 349 GHz (Sanna *et al.* 2021). For clarity, this image has been rotated by –33° with respect to the equatorial reference frame, in order to display the disk plane and outflow axis along the horizontal and vertical directions, respectively.

Thanks to powerful facilities like ALMA, one can nowadays measure temperature profiles and column (and volume) densities at angular scales comparable to maser cloudlets. For instance, we accurately derived the physical conditions per beam (of few 100 au) across the color map in Fig 4 by fitting methyl-cyanide ($CH_3CN$) emission lines (insets),

https://doi.org/10.1017/S1743921323002594 Published online by Cambridge University Press

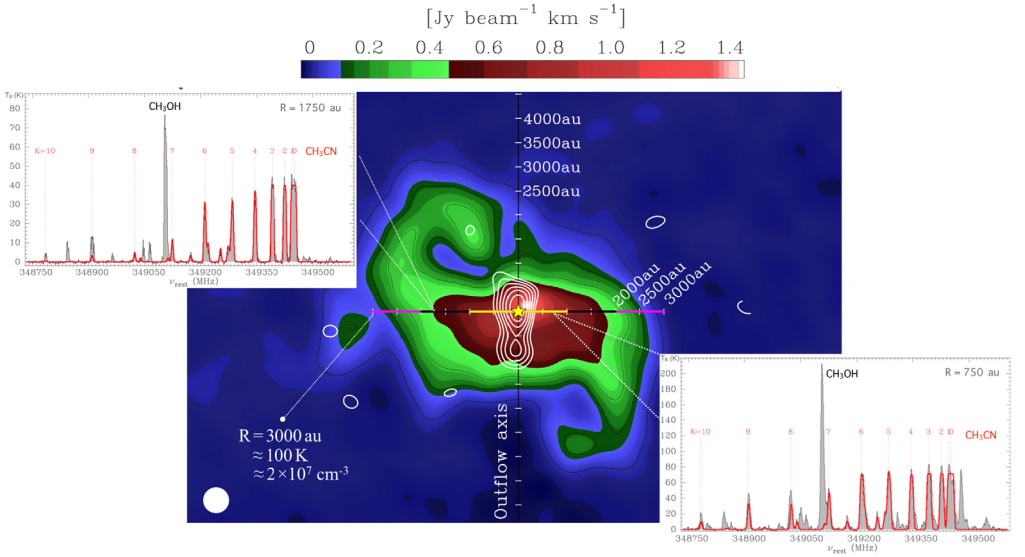


**Figure 4.** Appearance of the disk-like structure (color map) around the most massive object (star symbol) in the star-forming region, G023.01–00.4, as seen by ALMA through $CH_3OH$ emission at 349.107 GHz (synthesized beam on the bottom left). The equatorial plane of the disk-like emission is drawn from the star along the horizontal axis up to radii of 3000 au, with white ticks at steps of 500 au. White contours along the vertical axis draw the radio thermal jet emission imaged with the VLA at 44 GHz, with comparable angular resolution than ALMA. As an example, insets show two ALMA spectra taken along the disk plane at different distances of 1750 au and 750 au from the central star. These spectra were used to derive the physical conditions of local gas (indicated for a radius of 3000 au), by fitting the line emission from the $CH_3CN$ K-ladder (red profile). Adapted from Sanna *et al.* 2021.

inferring that gas is warmed up to temperatures of 90-100 K at a projected distance (R) of 3000 au from the star. At this distance, gas and dust condense to particle densities of approximately $10^7$ cm$^{-3}$. Moving closer to the central star, the temperature rises exponentially ($R^{-0.4}$) to almost 300 K at a projected distance of 250 au, where densities reach several $10^9$ cm$^{-3}$ (Sanna *et al.* 2021).

In Fig. 5, we present the same ALMA image with overlaid the positions of individual maser cloudlets emitting at 6.7 GHz, as we measured in 2010 and registered for the secular motion (Sanna *et al.* 2010b). Their distance with respect to the young star covers a range of projected radii from 2000 au down to about 500 au, avoiding the inner densest regions and in agreement with a quenching threshold of the order of $10^8$ cm$^{-3}$. This example shows we are in a position to draw detailed comparisons of maser positions with thermal line emission and to eventually constrain very local maser conditions. Therefore, we prompt our community for increasing the number of similar studies in the next years, which is crucial information for improving current models of maser excitation.

Another example of the synergies between interferometric observations in the millimeter and centimeter windows is related to the comparison of maser lines from the same molecular species, that are are spatially coincident but are emitted at different frequencies.

In Fig 4, we show two ALMA spectra near 349 GHz extracted at projected distances of 1750 au and 750 au from the central star. The red profile draws the best-fitted spectrum of the methyl-cyanid emission used to derive the local gas conditions, with the lower-energy (K = 1–4) lines that are optically-thick and set the maximum brightness temperature expected under local thermodynamic equilibrium. Notably, at the center of the bands a

https://doi.org/10.1017/S1743921323002594 Published online by Cambridge University Press

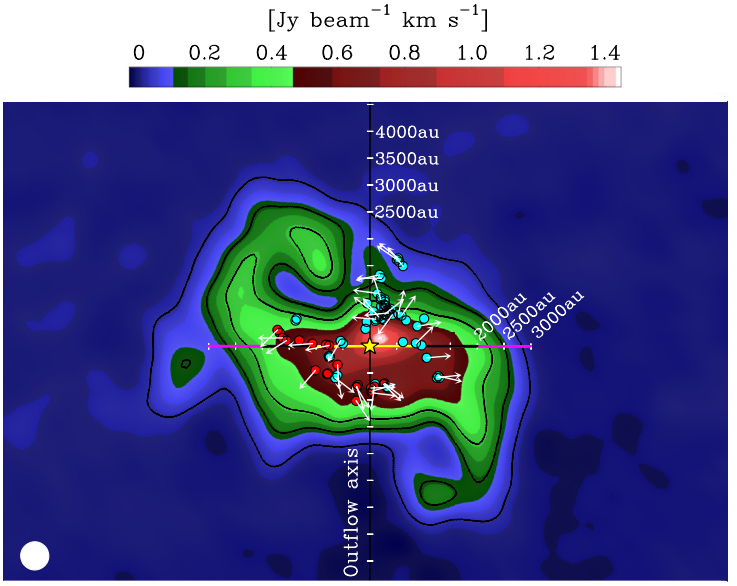


**Figure 5.** Same background color map as in Fig. 4 with overlaid the VLBI maser emission of methanol at 6.7 GHz (dots). Red and cyan dots indicate red- and blue-shifted line-of-sight maser velocities, respectively, and white arrows draw the local direction of the proper motion vector for individual maser cloudlets. Adapted from Sanna *et al.* 2021.

methanol line with an excitation temperature of 260 K, similar to the $CH_3CN$ K = 4 line, stands much brighter, and its emission was indeed used for the background color map.

Since methanol and methyl-cyanid are thought to be well mixed with each other for gas densities above $10^6$ cm$^{-3}$, these spectra can be interpreted as evidence that the methanol emission at 349.107 GHz has a strong maser contribution, in addition to a plateau of thermal emission. Moreover, this behavior is observable up to distances of about 2000 au from the central star, similar to the 6.7 GHz maser distribution. It is also worth noting that the same millimeter methanol maser was reported to be excited in another massive young star by Zinchenko *et al.* (2018). Following these findings, we further prompt our community to increase the number of millimeter masers studies, whose combination with their known centimeter counterparts can provide a unique information to improve both, maser models and our definition of "disk-like" environment.

### 3.2. *Expanding motions vs. infalling motions*

A final remark concerns the information coming from the analysis of full-space motions of methanol masers. From a kinematic point of view, the most characteristic pattern of a disk-like structure is expected to be rotation about an outflow axis, although a rotational component can be mixed to expanding or infalling gas motions depending on the spatial region where maser are excited. Is there any clear indication coming from maser proper motions so far?

As an example, we refer again to the star-forming region, G023.01–00.41. In Fig 5, the full-space motions of methanol masers can be decomposed in two main components, one along the line-of-sight and one on the plane of the sky. On the one hand, the former component bear the signs of (sub-Keplerian) rotation, with the redshifted and blueshifted masers to the west and east of the star position, respectively. On the other hand, the latter component traces gas pushed away from the central source, both along the disk plane and

https://doi.org/10.1017/S1743921323002594 Published online by Cambridge University Press

the perpendicular direction. This scenario of gas slowly expanding (and rotating) near a young star has been recurrently observed via 6.7 GHz maser proper motion measurements (e.g., Sanna *et al.* 2010b; Moscadelli *et al.* 2011a, 2013; Bartkiewicz *et al.* 2020).

Then, are 6.7 GHz masers preferentially tracing gas expansion? Or, alternatively, can 6.7 GHz masers be also associated with gas infall and, if yes, under which conditions? Interestingly, two examples exist where the full-space motions of methanol masers provide evidence of gas infall towards the central star, in the star-forming regions AFGL 5142 and Cepheus A (Goddi *et al.* 2011; Sugiyama *et al.* 2014; Sanna *et al.* 2017). Although this scenario seems less common so far, our observations might be biased towards more luminous and likely more evolved targets, where mass accretion (thus gas infall) might be reduced significantly.

Nevertheless, the chance of a direct measurement of gas infall by means of 6.7 GHz methanol masers appears very promising and would provide an extremely valuable information to the star formation community (otherwise difficult to obtain). For this reason, we prompt our community to search for methanol maser targets with evidence of infall in the next years, to increase the number of detections and eventually allow a detailed statistical analysis.

## References

Bartkiewicz, A., Sanna, A., Szymczak, M., *et al.* 2020, *A&A*, 637, A15
Cragg, D. M., Johns, K. P., Godfrey, P. D., *et al.* 1992, *MNRAS*, 259, 203
Cragg, D. M., Sobolev, A. M., & Godfrey, P. D. 2005, *MNRAS*, 360, 533
Elitzur, M., Hollenbach, D. J., & McKee, C. F. 1989, *ApJ*, 346, 983
Elitzur, M., Hollenbach, D. J., & McKee, C. F. 1992, *ApJ*, 394, 221
Genzel, R., Reid, M. J., Moran, J. M., *et al.* 1981, *ApJ*, 244, 884
Goddi, C., Moscadelli, L., & Sanna, A. 2011, *A&A*, 535, L8
Gwinn, C. R., Moran, J. M., & Reid, M. J. 1992, *ApJ*, 393, 149
Hollenbach, D., Elitzur, M., & McKee, C. F. 2013, *ApJ*, 773, 70
Kaufman, M. J. & Neufeld, D. A. 1996, *ApJ*, 456, 250
Menten, K. M. 1991, *ApJL*, 380, L75
Minier, V., Booth, R. S., & Conway, J. E. 2002, *A&A*, 383, 614
Moscadelli, L., Cesaroni, R., Rioja, M. J., *et al.* 2011, *A&A*, 526, A66
Moscadelli, L., Sanna, A., & Goddi, C. 2011, *A&A*, 536, A38
Moscadelli, L., Li, J. J., Cesaroni, R., *et al.* 2013, *A&A*, 549, A122
Moscadelli, L., Sánchez-Monge, Á., Goddi, C., *et al.* 2016, *A&A*, 585, A71
Moscadelli, L., Sanna, A., Goddi, C., *et al.* 2019, *A&A*, 631, A74
Moscadelli, L., Sanna, A., Goddi, C., *et al.* 2020, *A&A*, 635, A118
Moscadelli, L., Sanna, A., Beuther, H., *et al.* 2022, *Nature Astronomy*, 6, 1068
Reid, M. J., Menten, K. M., Brunthaler, A., *et al.* 2014, *ApJ*, 783, 130
Sanna, A., Moscadelli, L., Cesaroni, R., *et al.* 2010, *A&A*, 517, A71
Sanna, A., Moscadelli, L., Cesaroni, R., *et al.* 2010, *A&A*, 517, A78
Sanna, A., Moscadelli, L., Surcis, G., *et al.* 2017, *A&A*, 603, A94
Sanna, A., Moscadelli, L., Goddi, C., *et al.* 2018, *A&A*, 619, A107
Sanna, A., Moscadelli, L., Goddi, C., *et al.* 2019, *A&A*, 623, L3
Sanna, A., Giannetti, A., Bonfand, M., *et al.* 2021, *A&A*, 655, A72
Sobolev, A. M., Cragg, D. M., & Godfrey, P. D. 1997, *A&A*, 324, 211
Sugiyama, K., Fujisawa, K., Doi, A., *et al.* 2014, *A&A*, 562, A82
Zinchenko, I., Liu, S.-Y., Su, Y.-N., *et al.* 2018, *IAU Symposium*, 332, 270

https://doi.org/10.1017/S1743921323002594 Published online by Cambridge University Press